



Contents lists available at ScienceDirect

Bioorganic & Medicinal Chemistry Letters

journal homepage: www.elsevier.com/locate/bmcl

(1,2,3-Triazol-4-yl)benzenamines: Synthesis and activity against VEGF receptors 1 and 2

Alexander S. Kiselyov^{a,*}, Marina Semenova^b, Victor V. Semenov^c^a deCODE, 2501 Davey Road, Woodridge, IL 60517, USA^b Institute of Developmental Biology, RAS, 26 Vavilov Str., 119334 Moscow, Russia^c Zelinsky Institute of Organic Chemistry, RAS, 47 Leninsky Prospect, 117913 Moscow, Russia

ARTICLE INFO

Article history:

Received 18 December 2008

Revised 15 January 2009

Accepted 15 January 2009

Available online 20 January 2009

Keywords:

Angiogenesis

ATP-competitive kinase inhibitors

Vascular endothelial growth factor receptor

2

VEGFR-2

(1,2,3-Triazol-4-yl) benzenamines

ABSTRACT

Derivatives of (1,2,3-triazol-4-yl)benzenamines are described as potent and ATP-competitive inhibitors of vascular endothelial growth factor receptors I and II (VEGFR-1/2). A number of compounds exhibited VEGFR-2 and VEGFR-1 inhibitory activity comparable to that of VatalanibTM in both HTRF enzymatic and cellular assays.

© 2009 Elsevier Ltd. All rights reserved.

Anti-angiogenesis agents that target malignant vasculature are of considerable interest due to their perceived potential to target tumor resistance towards chemo- and radiotherapy.^{1–3} Vascular endothelial growth factors (VEGFs) and their respective family of receptor tyrosine kinases (VEGFRs) are key proteins modulating angiogenesis, the formation of new vasculature from an existing vascular network.^{4–10} These include VEGFR-1 (Flt-1) and VEGFR-2 (Kinase Insert Domain Receptor (KDR) or flk1).^{10–13} VEGFR-2 is the major positive signal transducer for endothelial cell proliferation and differentiation.¹¹ There has been considerable evidence, including clinical observations, that the abnormal angiogenesis is implicated in a number of diseases including rheumatoid arthritis, inflammation, cancer, degenerative eye conditions and others.^{12,13} Several molecules have been successfully used for sequestering VEGF leading to a signal blockade via VEGF receptors and, subsequently to an inhibition of malignant angiogenesis. One of the agents reportedly working via this mechanism is AvastinTM.¹⁴ A number of small-molecule inhibitors that affect VEGF/VEGFR signaling by directly competing with the intracellular ATP binding site of the respective intracellular kinase domain have been reported. These include VatalanibTM (**A**),¹⁵ BAY579352 (**B**),¹⁶ and the isosteric anthranil amide derivatives **C**¹⁷ and AMG-706 (**D**).¹⁸ Intramolecular hydrogen bonding in **C** and **D** was suggested^{17–19} to be

responsible for the optimal spatial orientation of the pharmacophore pieces (Fig. 1).²⁰

The essential pharmacophore elements for the VEGFR-2 activity of phthalazine-based molecules and their analogues (**A–D**) include²⁰ (i) [6,6]fused (or related) aromatic system; (ii) *para*- or 3,4-*di*-substituted aniline function in position 1 of the phthalazine core; (iii) hydrogen bond acceptor (Lewis' base: lone pair(s) of a nitrogen- or oxygen atom(s)) attached to position 4 via an appropriate linker (aryl or fused aryl group). In this communication, we expand upon our initial findings^{19,20} and disclose potent inhibitors of VEGFR-2 kinase based on (1,2,3-triazol-4-yl)benzenamines. We reasoned that this template could provide for the both proper pharmacophore arrangement and favorable in vitro/cellular potency of the resulting molecules.

A series of (1,2,3-triazol-4-yl)benzenamines **3–28** (Scheme 1, Table 1) were synthesized as described in Scheme 1.²¹ Reaction sequence involved the initial formation of enamines **1** from the respective *o*-nitrotoluene derivatives (R = H, Cl, CF₃) in a 79–92% yield. Pharmacophore group Ar¹ was introduced by the 1,3-dipolar cycloaddition reaction of **1** with a series of aryl azides in MeCN at reflux to afford the key intermediate nitroaryl 1,2,3-triazoles **2** in a 56–84% isolated yields. Compounds **2** were further converted to anilines followed by the reductive amination of these in order to introduce the Ar² group. Using this methodology, we have prepared a library of 25 derivatives **3–28** (51–72% yields from **2**, 24–52% overall yields from nitrotoluenes).

* Corresponding author. Tel.: +1 630 783 4900.

E-mail address: akiselyov@decode.com (A.S. Kiselyov).

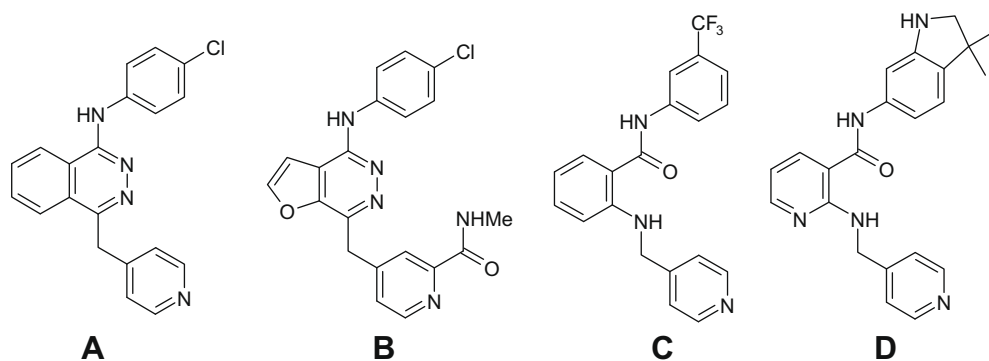
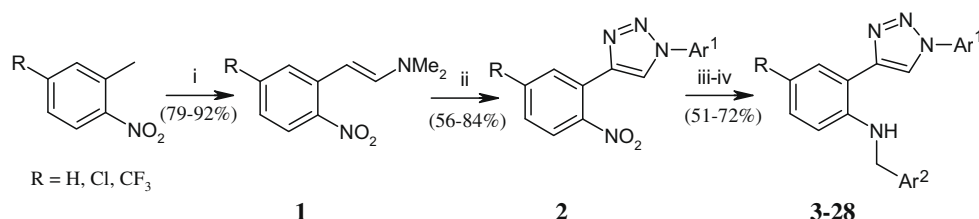


Figure 1. Selected Inhibitors of VEGFR-2.



Scheme 1. Synthesis of (1,2,3-triazol-4-yl)benzenamines **3–28**. Reagents and conditions: (i) $\text{Me}_2\text{NCH}(\text{OMe})_2$, DMF, reflux, 40 h; (ii) Ar^1N_3 , MeCN, reflux, 48 h; (iii) Fe, AcOH aq, reflux, 6 h; (iv) Ar^2CHO , iPrOH, reflux, 5 min; NaBH_4 , iPrOH.

Compounds (**3–28**, Table 1) were first tested in vitro against VEGFR-2²² measuring their ability to inhibit phosphorylation of a biotinylated-polypeptide substrate (p-GAT, CIS Bio International) in a homogenous time-resolved fluorescence (HTRF) assay at an ATP concentration of 2 μM . The results were reported as a 50% inhibition concentration value (IC_{50}). VEGFR-2 inhibitors VatalanibTM and **C** (Fig. 1) were used as internal standards.

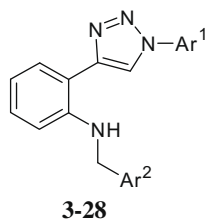
As can be seen from Table 1, several (1,2,3-triazol-4-yl)benzenamines exhibited good inhibitory activity against VEGFR-2 (**bolded** entries).²² By varying substituents at both Ar^1 and Ar^2 , it was possible to modulate compounds' potency against the enzyme. Notably, 5-substitution at the core benzene ring in **3–28** (e.g., $\text{R} = 5\text{-Cl}$, 5-CF_3) was not tolerated. In studying SAR of the **triazole** pharmacophore (Ar^1), we found that compounds featuring *meta*-substituted Ar^1 , as exemplified by *m*-Cl (**3**), *m*- CF_3 - (**6**), *m*- OCF_3 (**9**), *m*-iPr (**13**) displayed sound potency against VEGFR-2 with the IC_{50} values of 51–110 nM. *Para*-substitution in this portion of the molecule was tolerated, however the respective analogues were >4-fold less active against the enzyme (Table 1, compare **3** and **10**, **6** and **11**, **9** and **12**). In order to further explore steric requirements for the Ar^1 substituent, we prepared a series of (1,2,3-triazol-4-yl)benzenamines featuring both heterocyclic (Table 1, **16**, **17**) and disubstituted Ar^1 functionalities (**18–22**). 2-(Quinoliny) (**16**) and 5-(indazolyl) (**17**) Ar^1 groups displayed deleterious effect on the overall activity of resulting molecules against the kinase. Derivatives featuring 3,4-disubstituted aryl groups featured somewhat reduced potency when compared to the respective mono-substituted *meta*-derivatives (compare **6**, **18** and **21**). These facts suggest presence of a relatively tight hydrophobic pocket in the binding site of VEGFR-2 (vide supra).

In the next series of experiments, we optimized the **aniline** substituent Ar^2 (Table 1, entries **3–8**, **23–28**). Similar to the earlier findings,^{19,20} 4-pyridyl group was present in the most active molecules. 4-Quinoliny derivatives (**26**, **27**) displayed diminished activity against VEGFR-2, even when endowed with the optimized Ar^1 functionality. 4-Imidazole derivative **28** was inactive. The com-

bined SAR data indicated that (i) substitution pattern on the Ar^1 group of the triazole (compare **3** and **10**, **6** and **11**, **9** and **12**) and (ii) nature of the aniline substituent Ar^2 (compare **3**, **4** and **5**, **23–28**) were critical to the VEGFR-2 inhibitory activity of these new series. In addition, 5-substitution of the central aromatic core was not tolerated.

Compounds **3–28** were also tested in HTRF format against VEGFR-1.²² The results in Table 1 suggest that all VEGFR-2 active (1,2,3-triazol-4-yl)benzenamine derivatives (e.g., **3**, **6**, **9**, **13**, **21**, **26**, **27**) consistently led to good activity against VEGFR-1 with the IC_{50} values in 66–210 nM range for the most potent compounds. This outcome could be of benefit in the clinical setting as both receptors are reported to mediate VEGF signaling in the aberrant angiogenesis.^{1–5,20} Further screening of **3–28** against a number of other receptor (IGF1R, InR, FGFR1, Flt3, EGFR, ErbB2, c-Met, Ron) and cytosolic (PKA, GSK3 β , bcr-Abl, bcr-AblT315, Cdk1/2, Src, Auroras A and B, Plk1) kinases in HTRF format indicated no significant cross reactivity (PI < 30%, triplicate measurements) at a concentration of 10 μM .

In order to further expand the utility of triazole scaffold, we have prepared a series of 1*H*-1,2,3-triazole-4-carboxamides **31–34** as shown on Scheme 2. Specifically, amides of cyanoacetic acid (**29**) underwent cyclization with benzyl azide under basic conditions to furnish the key *N*-benzyltriazole intermediates **30**. *N*-Benzyl group in **30** was removed by hydrogenation over Pd/C followed by the reductive amination of resulting NH-triazoles to yield the targeted molecules **31–34** in a 24–47% overall yields. Disappointingly, these molecules did not display any significant activity against VEGFR-2 or VEGFR-1 kinases. For example, compounds **31** and **33** featuring optimized pharmacophores (Table 1, see compounds **3** and **6**) showed IC_{50} values of ca. 5–7 μM against VEGFR-2 and were essentially inactive in the cell-based assay. Compounds **32** and **34** also did not show any activity against the kinases ($\text{IC}_{50} > 10 \mu\text{M}$). We explained this outcome by the considerably different pharmacophore arrangement in the aryltriazole series exemplified by **3** and in 3,4-substituted triazoles (**31–34**).

Table 1Activity of (1,2,3-triazol-4-yl)benzenamines **3–28** against VEGFR-2 and VEGFR-1 kinase in vitro and in cell-based assays.

Compound	Ar ¹	Ar ²	VEGFR-2, enzymatic, IC ₅₀ ^a (μM)	VEGFR-1, enzymatic, IC ₅₀ ^a (μM)	VEGFR-2, cell-based ELISA, IC ₅₀ ^{a,b,c} (μM)
A, PTK787			0.054 ± 0.006	0.14 ± 0.02	0.021 ± 0.03
Vatalanib™			(0.042 ± 0.003) ^b	(0.11 ± 0.03) ^b	(0.016 ± 0.001) ^b
C			0.032 ± 0.005	0.17 ± 0.05	0.09 ± 0.01
			(0.023 ± 0.006) ^b	(0.130 ± 0.081) ^b	(0.0012 ± 0.0002) ^b
3	3-Cl-(C₆H₄)	4-Pyridine	0.087 ± 0.011	0.13 ± 0.025	0.16 ± 0.05^d
4	3-Cl-(C ₆ H ₄)	3-Pyridine	4.23 ± 0.51	>10	>10
5	3-Cl-(C ₆ H ₄)	2-Pyridine	>10	>10	>10
6	3-F₃C-(C₆H₄)	4-Pyridine	0.051 ± 0.05	0.066 ± 0.07	0.096 ± 0.14
7	3-F ₃ C(C ₆ H ₄)	3-Pyridine	>10	>10	>10
8	3-F ₃ C(C ₆ H ₄)	2-Pyridine	>10	>10	>10
9	3-F₃CO(C₆H₄)	4-Pyridine	0.066 ± 0.005	0.072 ± 0.01	0.085 ± 0.02
10	4-Cl-(C ₆ H ₄)	4-Pyridine	0.39 ± 0.09	0.13 ± 0.025	0.27 ± 0.01 ^d
11	4-F ₃ C-(C ₆ H ₄)	4-Pyridine	0.59 ± 0.13	0.66 ± 0.12	1.92 ± 0.36
12	4-F ₃ CO(C ₆ H ₄)	4-Pyridine	1.22 ± 0.26	1.13 ± 0.19	3.11 ± 0.45
13	3-<i>i</i>Pr-(C₆H₄)	4-Pyridine	0.11 ± 0.01	0.13 ± 0.03	0.15 ± 0.05
14	3- <i>t</i> Bu-(C ₆ H ₄)	4-Pyridine	0.27 ± 0.05	0.25 ± 0.08	0.33 ± 0.11
15	4- <i>t</i> Bu-(C ₆ H ₄)	4-Pyridine	0.61 ± 0.09	0.53 ± 0.07	1.63 ± 0.34
16	2-(Quinoliny)	4-Pyridine	0.77 ± 0.18	0.64 ± 0.11	1.19 ± 0.22
17	5-(Indazolyl)	4-Pyridine	0.68 ± 0.14	0.65 ± 0.13	2.33 ± 0.28
18	3-F ₃ C,4-Cl(C ₆ H ₄)	4-Pyridine	0.44 ± 0.11	0.51 ± 0.10	0.78 ± 0.16
19	3-Cl,4-F ₃ C(C ₆ H ₄)	4-Pyridine	0.93 ± 0.18	1.13 ± 0.21	2.92 ± 0.44
20	3,4-di-Cl(C ₆ H ₄)	4-Pyridine	0.63 ± 0.15	0.65 ± 0.12	1.47 ± 0.27
21	4-Me-3-F₃C(C₆H₃)	4-Pyridine	0.14 ± 0.03	0.11 ± 0.02	0.18 ± 0.03
22	3-Me-4-F ₃ C(C ₆ H ₃)	4-Pyridine	0.98 ± 0.21	0.86 ± 0.20	2.02 ± 0.35
23	3-Cl-(C ₆ H ₄)	3,4-di-F-(C ₆ H ₃)	>10	>10	>10
24	3-Cl-(C ₆ H ₄)	5-Piperonyl	>10	>10	>10
25	3-CF ₃ -(C ₆ H ₄)	5-Piperonyl	>10	>10	>10
26	3-Cl-(C₆H₄)	4-Quinolyl	0.19 ± 0.08	0.17 ± 0.02	0.27 ± 0.06
27	3-F₃C(C₆H₄)	4-Quinolyl	0.16 ± 0.04	0.21 ± 0.05	0.31 ± 0.09
28	3-Cl-(C ₆ H ₄)	4-Imidazolo	>10	>10	>10

^a IC₅₀ values were determined from the logarithmic concentration-inhibition point (10 points).²² The important values are given as the mean of at least two duplicate experiments.

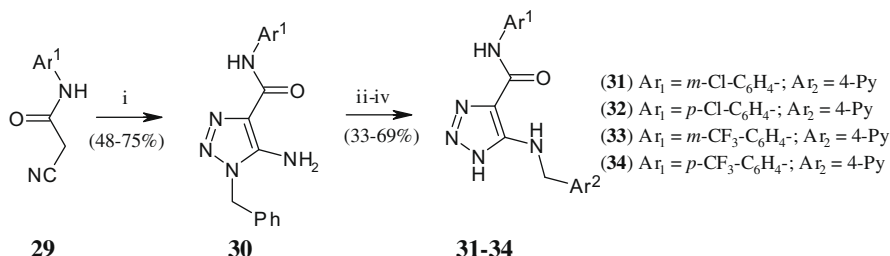
^b Lit. IC₅₀ values, as measured at 8 μM ATP.^{15,17}

^c Lit. data correspond to the inhibition of VEGF-induced phosphorylation of VEGFR-2 in CHO cells.^{15,17}

^d Molecules with best enzymatic and cellular potencies against VEGFR-2 are bolded.^{22,23}

We reasoned that proper alignment of the lower portion of the molecule, namely nitrogen atoms (Lewis' base, hydrogen bond acceptors) of 4-pyridyl or 4-quinolyl groups (Table 1, e.g., **3** and **30**) with the Arg1302 moiety in the ATP-binding pocket of VEGFR-2 is required for the activity. Docking of **3** into the cocrystal structure 2P2I of a biphenyl analogue **D** with VEGFR2 revealed that the 1,2,3-triazole function of **3** is accommodated in a well-defined binding pocket lined up with Ala866 and Lys868. This allows for a better fit of a *meta*-substituted aryl moiety in the hydrophobic

pocket of the ATP-binding site of the kinase.^{19,20} There is a possibility for it to displace a water molecule from the active site of kinase (Fig. 2a). In addition, we concluded that *N*-atoms of the triazole ring could make a contact with the backbone NH of Arg1046. These features are absent in the 1,2,3-triazole derivative **31**. Lack of activity for **31–34** likely results from the improper alignment of its amide substituent in the hydrophobic pocket of the kinase. Minimization studies suggest that the positioning of Ar¹ pharmacophore for **3** and **31** differs considerably (Fig. 2b). In addition,



Scheme 2. Reagents and conditions: (i) PhCH₂N₃, KOH, EtOH, 80 °C, 1 h; (ii) H₂, Pd/C, 80 °C, 4 h; (iii) Ar²CHO, 4Å mol. sieves, benzene, 90 °C, 4 h; (iv) NaBH₄, iPrOH, 100 °C, 2 h.

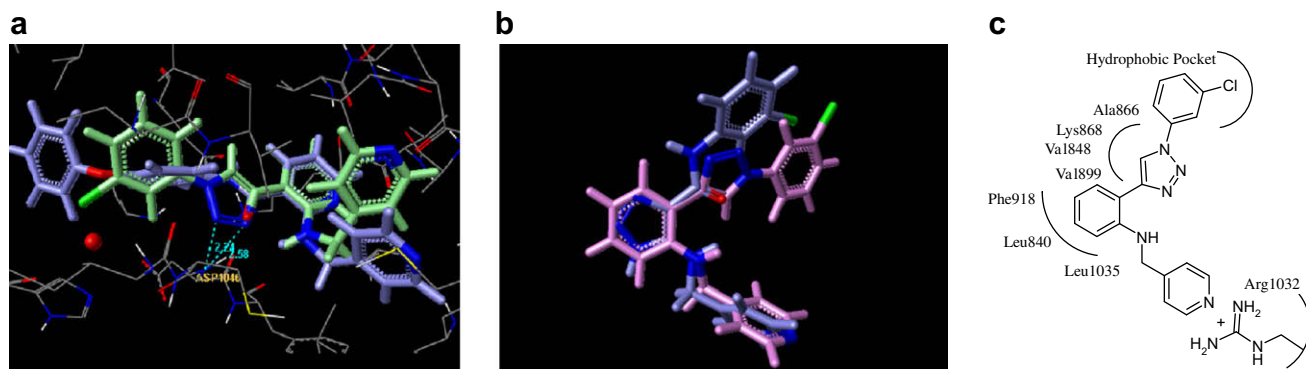


Figure 2. Structural overlap between (a) **3** (green) and biphenyl analogue of **D** (blue) from the 2P2 l co-crystal structure with VEGFR; (b) structural overlap of compounds **3** and **31**; (c) pharmacophore hypothesis for the mode of binding of (1,2,3-triazol-4-yl)benzenamine **3** within the ATP binding pocket of VEGFR-2. Central aromatic ring is surrounded by *Leu840*, *Val848*, *Val899*, *Phe918* and *Leu1035*. The amide is in close proximity with the *Ala 866* and *Lys868*, and pyridine nitrogen is near *Arg1032*.

Table 2

Compounds **3**, **6** and **13** are ATP-competitive inhibitors of VEGFR-2.

Compound	K_i at IC_{50} (μM)	K_i at IC_{90} (μM)
3	0.12	0.11
6	0.09	0.08
13	0.16	0.14

acidic proton of the pyrrole NH in the triazole ring of **31–34** may cause unfavorable interactions in the binding pocket lined up with *Leu840*, *Phe918* and *Leu1035* residues. Observed structure–activity relationship of the novel (1,2,3-triazol-4-yl)benzenamines **3–28** are in line with the proposed pharmacophore hypothesis (Fig. 2c).

Active in vitro inhibitors of VEGFR-2 were further characterized in a cell-based phosphorylation ELISA assay (Table 1).²³ In general, good in vitro-to-cell based activity correlation has been found for these compounds. In our hands, the best compounds displayed 85–310 nM activity in inhibiting cell-based phosphorylation of VEGFR-2. Further, competition assays were conducted for the selected molecules with varying concentration (0–100 μM) of ATP. Specifically, five different concentrations of ³²P ATP were incubated with VEGFR-2 along with varying concentrations (absence, IC_{50} , IC_{90}) of the inhibitors **3**, **6** and **13** for 45 min at RT. A double reciprocal graph of the degree of phosphorylation (1/cpm) against ATP-concentration (1/[ATP]) was plotted. The data were analyzed by a non-linear least-squares program to determine kinetic parameters using GraphPad software. Determined K_i values for the three selected compounds are listed in Table 2. These data suggest an ATP-competitive mechanism for the interaction of these inhibitors with VEGFR-2.

In summary, we have described a series of (1,2,3-triazol-4-yl)benzenamines as potent inhibitors of both VEGFR-2 and VEGFR-1 receptors. Enzymatic and cellular activities of representative molecules are comparable to the clinical candidates VatalanibTM and AMG-706. This outcome could be of benefit in the clinical setting as both receptors are reported to mediate VEGF signaling in the angiogenesis. Notably, 1H-1,2,3-triazole-4-carboxamide analogues did not show any appreciable activity against the kinases suggesting strict electronic and spatial demands for the proper alignment of ligand in a binding pocket of the enzymes.

References and notes

- Bailar, J. C., III; Gornick, H. L. *N. Engl. J. Med.* **1997**, 336, 1569.
- Boehm, T.; Folkman, J.; Browder, T. *Nature* **1997**, 390, 404.
- Risau, W. *Nature* **1997**, 386, 671.
- Klagsbrun, M.; Moses, M. A. *Chem. Biol.* **1999**, 6, R217.
- Hanahan, D.; Folkman, J. *Cell* **1996**, 86, 353.
- Olsson, A.-K.; Dimberg, A.; Kreuger, J.; Claesson-Welsh, L. *Nat. Rev. Mol. Cell Biol.* **2006**, 5, 359.
- Zachary, I. *Biochem. Soc. Trans.* **2003**, 31, 1171.
- Perona, R. *Clin. Transl. Oncol.* **2006**, 8, 77.
- Jin, T.; Nakatani, H.; Taguchi, T. *World J. Gastroenterol.* **2006**, 12, 703.
- Itakura, J.; Ishiwata, T.; Shen, B. *Int. J. Cancer* **2000**, 85, 27.
- Saario, A.; Karpanen, T.; Alitalo, K. *Oncogene* **2000**, 19, 6122.
- Ferrara, N.; Hillan, K. J.; Gerber, H. P.; Novotny, W. *Nature Rev. Drug Discov.* **2004**, 3, 391.
- Fine, S. L.; Martin, D. F.; Kirkpatrick, P. *Nature Rev. Drug Disc.* **2005**, 4, 187.
- Culy, C. *Drugs Today* **2005**, 41, 23.
- Bold, G.; Altmann, K.-H.; Jorg, F.; Lang, M.; Manley, P. W.; Traxler, P.; Wietfeld, B.; Bruggen, J.; Buchdunger, E.; Cozens, R.; Ferrari, S.; Pascal, F.; Hofmann, F.; Martiny-Baron, G.; Mestan, J.; Rosel, J.; Sills, M.; Stover, D.; Acemoglu, F.; Boss, E.; Emmenegger, R.; Lasser, L.; Masso, E.; Roth, R.; Schlachter, C.; Vetterli, W.; Wyss, D.; Wood, J. M. *J. Med. Chem.* **2000**, 43, 2310.
- Chang, Y.S.; Cortes, C.; Polony, B. *Proc. Am. Assoc. Cancer Res. (AACR)* **2005**, 46, Abstr 2030.
- Manley, P. W.; Furet, P.; Bold, G.; Bruggen, J.; Mestan, J.; Meyer, T.; Schnell, C.; Wood, J. J. *Med. Chem.* **2002**, 45, 5697.
- Kaufman, S.; Starnes, C.; Coxon, A. *Proc. Am. Assoc. Cancer Res. (AACR)* **2006**, 47, Abstr 3792.
- Kiselyov, A. S.; Piatnitski, L. E.; Samet, A. V.; Kisly, V. P.; Semenov, V. V. *Bioorg. Med. Chem. Lett.* **2007**, 17, 1369, and references cited therein.
- Kiselyov, A. S.; Balakin, K.; Tkachenko, S. E. *Expert Opin. Invest. Drugs* **2007**, 16, 83.
- Analytical data for selected molecules: 2-(1-(3-chlorophenyl)-1H-1,2,3-triazol-4-yl)-N-(pyridin-4-ylmethyl)benzenamine (**3**): mp 174–175 °C; ¹H NMR (400 MHz, DMSO-*d*₆) δ , ppm: 4.28 (d, *J* = 8.0 Hz, 2H), 6.50 (d, *J* = 7.2 Hz, 1H), 6.61 (br s, exch D₂O, 1H, NH), 6.93 (m, 1H), 7.06 (d, *J* = 7.6 Hz, 1H), 7.22 (m, 1H), 7.28 (d, *J* = 7.6 Hz, 1H), 7.35 (s, 1H), 7.40 (m, 1H), 7.46 (d, *J* = 7.2 Hz, 2H), 7.94 (s, 1H), 8.55 (d, *J* = 7.2 Hz, 2H), 8.73 (d, *J* = 7.2 Hz, 1H); ¹³C NMR (100 MHz, DMSO-*d*₆) δ , ppm: 45.8, 109.6, 113.7, 118.0, 124.3, 125.6, 127.9, 128.2, 128.5, 129.4, 129.8, 132.1, 134.2, 134.7, 146.4, 147.4, 148.7, 150.1; ESI MS (*M*+1): 363, (*M*-1): 361. Elemental analysis: Calcd for C₂₀H₁₆ClN₅: C, 66.39; H, 4.46; N, 19.36. Found: C, 66.17; H, 4.58; N, 19.13.
- N-(Pyridin-4-ylmethyl)-2-(1-(3-(trifluoromethyl)phenyl)-1H-1,2,3-triazol-4-yl)benzenamine (**6**): mp 196–197 °C; ¹H NMR (400 MHz, DMSO-*d*₆) δ , ppm: 4.31 (d, *J* = 8.0 Hz, 2H), 6.48 (d, *J* = 7.2 Hz, 1H), 6.58 (br s, exch D₂O, 1H, NH), 6.94 (m, 1H), 7.21 (m, 1H), 7.29 (d, *J* = 8.0 Hz, 1H), 7.33 (s, 1H), 7.36–7.41 (m, 4H), 7.97 (s, 1H), 8.56 (d, *J* = 7.6 Hz, 2H), 8.78 (d, *J* = 7.2 Hz, 1H); ¹³C NMR (100 MHz, DMSO-*d*₆) δ , ppm: 46.1, 109.4, 117.9, 120.1, 124.0, 124.3, 125.3, 127.8, 128.6, 128.9, 129.1, 129.7, 130.7, 131.5, 133.4, 146.0, 147.9, 148.5, 150.1; ESI MS (*M*+1): 396, (*M*-1): 394. Elemental analysis: Calcd for C₂₁H₁₆F₃N₅: C, 63.79; H, 4.08; N, 17.71. Found: C, 63.52; H, 3.87; N, 17.49.
- 2-(1-(3-chlorophenyl)-1H-1,2,3-triazol-4-yl)-N-(quinolin-4-ylmethyl)benzenamine (**26**): mp 231–233 °C; ¹H NMR (400 MHz, DMSO-*d*₆) δ , ppm: 4.31 (d, *J* = 7.6 Hz, 2H), 6.49 (d, *J* = 7.2 Hz, 1H), 6.65 (br s, exch D₂O, 1H, NH), 6.91 (m, 1H), 7.03 (d, *J* = 7.6 Hz, 1H), 7.12 (d, *J* = 7.6 Hz, 1H), 7.18 (m, 1H), 7.28–7.30 (m, 2H), 7.42 (m, 1H), 7.54 (m, 1H), 7.68 (m, 1H), 7.98 (d, *J* = 7.6 Hz, 1H), 8.07 (s, 1H), 8.21 (d, *J* = 7.2 Hz, 1H), 8.71 (d, *J* = 7.2 Hz, 1H), 8.91 (d, *J* = 7.2 Hz, 1H); ¹³C NMR (100 MHz, DMSO-*d*₆) δ , ppm: 44.5, 109.4, 113.8, 118.1, 121.8, 124.3, 125.2, 126.2, 126.9, 127.5, 128.3, 128.9, 128.3, 129.1, 129.3, 129.8, 130.2, 130.6, 132.3, 134.2, 146.4, 146.6, 149.1, 150.8; ESI MS (*M*+1): 413, (*M*-1): 411; Elemental analysis: Calcd for C₂₄H₁₈ClN₅: C, 69.98; H, 4.40; N, 17.00. Found: C, 69.76; H, 4.28; N, 16.81.
- N-((1H-imidazol-4-yl)methyl)-2-(1-(3-chlorophenyl)-1H-1,2,3-triazol-4-yl)benzenamine (**28**): mp 163–164 °C; ¹H NMR (400 MHz, DMSO-*d*₆) δ , ppm: 4.30 (d, *J* = 7.6 Hz, 2H), 6.51 (d, *J* = 7.2 Hz, 1H), 6.59 (br s, exch D₂O, 1H, NH), 6.77 (s, 1H), 6.90 (m, 1H), 7.08 (d, *J* = 7.6 Hz, 1H), 7.21 (m, 1H), 7.29 (d, *J* = 7.6 Hz, 1H), 7.32 (s, 1H), 7.43 (m, 1H), 7.48 (s, 1H), 8.12 (s, 1H), 8.73 (d, *J* = 7.2 Hz, 1H), 12.9 (br s, exch D₂O, 1H, NH imidazole); ¹³C NMR (100 MHz, DMSO-*d*₆) δ , ppm: 43.9,

109.2, 113.6, 118.2, 120.2, 125.1, 127.6, 127.9, 128.5, 129.7, 130.2, 131.6, 132.2, 135.6, 134.4, 146.7, 148.1, 148.7; ESI MS (M+1): 352, (M-1): 350. Elemental analysis: Calcd for C₁₈H₁₅ClN₆: C, 61.63; H, 4.31; N, 23.96. Found: C, 61.38; H, 4.12, N, 23.69.

N-(3-Chlorophenyl)-5-(pyridin-4-ylmethylamino)-1*H*-1,2,3-triazole-4-carboxamide (**31**): mp 181–183 °C (decomp.); ¹H NMR (400 MHz, DMSO-*d*₆) δ, ppm: 4.31 (d, *J* = 8.0 Hz, 2H), 6.78 (br s, exch D₂O, 1H, NH), 7.13 (d, *J* = 7.6 Hz, 1H), 7.37 (m, 1H), 7.45 (d, *J* = 7.2 Hz, 2H), 7.78 (d, *J* = 7.6 Hz, 1H), 7.98 (s, 1H), 8.65 (d, *J* = 7.2 Hz, 2H), 10.20 (br s, exch D₂O, 1H, NH), 11.8 (s, exch D₂O, 1H, NH triazole); ¹³C NMR (100 MHz, DMSO-*d*₆) δ, ppm: 45.8, 119.6, 121.7, 124.4, 124.6, 124.9, 130.2, 133.9, 137.1, 142.9, 147.5, 150.2, 163.2; ESI MS (M + 1): 330, (M-1): 328; Elemental analysis: Calcd for C₁₅H₁₃ClN₆O: C, 54.80; H, 3.99; N, 25.56. Found: C, 54.59; H, 3.82, N, 25.38.

22. VEGFR tyrosine kinase inhibition is determined by measuring the phosphorylation level of poly-Glu-Ala-Tyr-biotin (pGAT-biotin) peptide in a Homogenous Time-Resolved Fluorescence (HTRF) assay. Into a black 96-well Costar plate is added 2 μl/well of 25X compound in 100% DMSO (final concentration in the 50 μl kinase reaction is typically 1 nM to 10 μM). Next, 38 μl of reaction buffer (25 mM Hepes pH 7.5, 5 mM MgCl₂, 5 mM MnCl₂, 2 mM DTT, 1 mg/ml BSA) containing 0.5 mmol pGAT-biotin and 3–4 ng KDR enzyme is added to each well. After 5–10 min preincubation, the kinase reaction is initiated by the addition of 10 μl of 10 μM ATP in reaction buffer, after which the plate is incubated at room temperature for 45 min. The reaction is stopped by addition of 50 μl of KF buffer, (50 mM Hepes, pH 7.5, 0.5 M KF, 1 mg/ml BSA) containing 100 mM EDTA and 0.36 μg/ml PY20 K (Eu-cryptate labeled anti-phosphotyrosine antibody, CIS bio international) is added and after an additional 2 h incubation at room temperature, the plate is read in a RUBYstar HTRF Reader.
23. Cell-based assay for VEGFR-2 inhibition:
(i) *Transfection of 293 cells with DNA expressing FGFR1/VEGFR-2 chimera*: A

chimeric construct containing the extracellular portion of FGFR1 and the intracellular portion of VEGFR-2 was transiently transfected into 293 adenovirus-transfected kidney cells. DNA for transfection was diluted to a 5 μg/ml final concentration in a serum-free medium and incubated at room temperature for 30 min with 40 μl/mL of Lipofectamine 2000, also in serum-free media. 250 μl of the Lipofectamine/DNA mixture was added to 293 cells suspended at 5 × 10⁵ cells/ml. Suspension (200 μl/well) was added to a 96-well plate and incubated overnight. Within 24 h, media was removed and 100 μl of media with 10% fetal bovine serum was added to the now adherent cells followed by an additional 24 h incubation. Test compounds were added to the individual wells (final DMSO concentration was 0.1%). Cells were lysed by re-suspension in 100 μl Lysis buffer (150 mM NaCl, 50 mM Hepes pH 7.5, 0.5% Triton X-100, 10 mM NaPPi, 50 mM NaF, 1 mM Na₃VO₄) and rocked for 1 h at 4 °C.

(ii) *ELISA for detection of tyrosine-phosphorylated chimeric receptor*: 96-well ELISA plates were coated using 100 μl/well of 10 μg/ml of αFGFR1 antibody, and incubated overnight at 4 °C. αFGFR1 was prepared in a buffer made with 16 ml of a 0.2 M Na₂CO₃ and 34 ml of a 0.2 M NaHCO₃ with pH adjusted to 9.6. Concurrent with lysis of the transfected cells, αFGFR1 coated ELISA plates were washed three times with PBS + 0.1% Tween 20, blocked by addition of 200 μl/well of a 3% BSA in PBS for 1 h and washed again. Eighty microliters lysate were then transferred to the coated and blocked wells and incubated for 1 h at 4 °C. The plates were washed three times with PBS + 0.1% Tween 20. To detect bound phosphorylated chimeric receptor, 100 μl/well of anti-phosphotyrosine antibodies (RC20:HRP, Transduction Laboratories) were added (final concentration 0.5 μg/ml in PBS) and incubated for 1 h. The plates were washed six times with PBS + 0.1% Tween 20. Enzymatic activity of HRP was detected by adding 50 μl/well of equal amounts of the Kirkegaard & Perry Laboratories (KPL) Substrate A and Substrate B. The reaction was stopped by addition of 50 μl/well of a 0.1 N H₂SO₄, absorbance was measured at 450 nm.